



Recent advancement of deep learning techniques for pneumonia prediction from chest X-ray image

ARTICLE INFO

Keywords:
 Pneumonia
 Chest X-ray
 Deep-Learning
 CNN
 Ensemble learning
 Transfer learning

ABSTRACT

Pneumonia is a life-threatening, acute lung infection found all over the world that mostly affects the lungs. Computer vision-related automatic detection algorithms are currently highly used in research areas like medical imaging. Deep learning algorithms have enabled some impressive improvements in medical diagnosis in recent years. This study provides a summary of a recently developed DL-based pneumonia diagnosis system as well as important details about the data sets used for the training and testing of those networks. Additionally, it emphasizes the ensemble learning and deep transfer learning methodologies as well as the many performance measurements created by researchers in this field. The most recent research publications are reviewed here and collected from different sources like Scopus, Google Scholar, PubMed, ResearchGate, and IEEE Xplore databases using the terms "Pneumonia", "Deep-Learning", "X-Ray" and "CNN". The most current works are organized according to a taxonomy for easier understanding. Lastly, we addressed the limitations in deploying deep learning methods to the detection of pneumonia and potential future developments in this field of study. This study aims to assist experts in select the most suitable and effective methods for pneumonia detection.

1. Introduction

In the last few decades, there have been major changes in the way global health works. Global warming, economic progress, and changes in people's lifestyles are all contributors to these shifts. Pneumonia is a very prevalent illness where the respiratory system is infected by bacteria or viruses [1]. The symptoms are quite similar to COVID-19 [2]. The alveoli fill with pus and fluid when a person has pneumonia, making breathing difficult and limiting oxygen intake. 7,40,180 children under the age of five died in 2019 due to pneumonia-related causes, per WHO data [3].

An easy, affordable, and widely used method of identifying lung infections is now X-ray images of the chest [4]. Expert radiographers can determine whether or not a chest X-ray shows signs of illness, such as lung cancer, pneumonia, or tuberculosis. Typically, viral pneumonia is less severe than bacterial pneumonia, particularly in children [5]. People with weakened immune systems are susceptible to developing fungal pneumonia. Chest X-rays are more frequently requested than other healthcare modalities due to its cost-effectiveness [6]. Each radiologist receives a huge number of readings each year due to the need for CXRs. Yet, both developed as well as developing nations are experiencing a radiologist shortage [7]. The situation can get worsen in developing nations due to a lack of qualified radiologists and environmental pollution. Timely diagnosis is also hampered by the extreme disparity between the population and the number of professionals in a particular region. Furthermore, CXRs have lesser resolution than CT scans and MRI, making it difficult for even experienced radiologists to effectively

interpret them. A computer-aided diagnostic technique system can assist medical professionals in making decisions by combining deep learning and computer vision and extracting patterns from chest X-ray images [8]. In computer-aided diagnostic systems, the data is first processed, after which the information is retrieved using algorithms or deep learning networks, the output is then assessed to determine if it is normal or disease-affected. Conventional computer-aided diagnostic systems have been successful in classifying lung illnesses from CXR images, but extracting feature from CXR images still involves considerable handcrafted techniques [9] (Khan et al., 2021). Many AI-based techniques were created to get around this limitation [10,11]. CNN architecture which has made significant advancements in a variety of pattern recognition tasks during the past ten years. However, CNN needs a significant amount of training data. In order to classify medical images using CNN pre-trained networks can be applied without further training or can develop a CNN model from scratch [12]. Deep learning-based algorithms, like U-Net, SegNet [13], Chexnet [14], and CardiacNet have recently been used for clinical image analysis.

Here is a summary of recent research about how chest X-rays can be used to find out if someone has pneumonia:

- Study and evaluation computational complexity, usability, and goodness of the algorithms used to identify pneumonia.
- Study and evaluation of the CXR image dataset's size, quality, and usability.
- Discusses and shows a comparison of the methods or algorithms used to identify pneumonia.

<https://doi.org/10.1016/j.hmedic.2024.100106>

Received 12 December 2023; Received in revised form 27 June 2024; Accepted 26 July 2024

Available online 30 July 2024

2949-9186/© 2024 The Authors. Published by Elsevier Ltd. This is an open access article under the CC BY license (<http://creativecommons.org/licenses/by/4.0/>).

- Provide healthcare practitioners and the research community future directions in light of the recent literature that could help them choose the best techniques, analyse the publicly available datasets, and finally understand the outcomes of this study.

Here is how the paper is structured: We provided a brief overview of pneumonia in [Section 1](#) while outlining the methodology in [Section 2](#) and [3](#). The entire publicly available dataset that was utilized to identify pneumonia is described in detail in [Section 4](#). In [Sections 5](#) and [6](#), we discussed pre-trained models with deep transfer learning and custom deep learning techniques that have been used to correctly identify pneumonia. In [Section 7](#), we discussed ensemble deep learning techniques proposed by different authors to effectively identify pneumonia. Finally, the paper digs into its conclusion.

2. Research methodology

The availability of information over the past few decades has provided a simpler way for researchers to construct a variety of deep learning architectures for diagnosing diseases such as cardiac disorders, skin cancer, COVID-19, pneumonia, etc. This study aims to provide an overview of pneumonia diagnosis using several deep learning architectures. We have divided our work into two sections: the first section discusses all the publicly available datasets used by different researchers in their proposed models, and the second section discusses deep learning-based techniques. The deep learning-based techniques have been divided into three parts: pre-trained models with deep transfer learning, custom deep learning techniques, and lastly ensemble deep learning techniques, shown in [Fig 1](#).

3. Deep learning in pneumonia detection

Deep learning approaches can learn from basic illustrations to solve or illustrate more complicated issues. Deep learning methods are widely used because they can make accurate representations and learn data deeply by stacking many layers one after the other. Deep learning techniques are frequently employed in healthcare systems, including biomedicine [15], smart healthcare [16], drug discovery [17], and medical image analysis [18].

Now-a-days, it has seen widespread implementation in computerized patient diagnosis for pneumonia. Basically, in deep learning technique has several steps like data collection, data preparation, model analysis and system evaluation. The general flow chart of deep learning techniques for pneumonia diagnosis is depicted in [Fig. 2](#). Patients diagnosed are assumed to participate in the data collection phase. For pneumonia detection lung X-ray image are taken. The data preparation step is necessary including noise removal, normalization, resizing, segmentation and augmentation to convert the data into appropriate format.

For future trials, the pre-processed dataset is divided into training, testing, and validation sets during the data partitioning step. For data partitioning, the cross-validation technique is commonly used. Models are developed using the training dataset and validated using the validation dataset. Lastly, the developed model's performance is evaluated using a test dataset. The feature extraction and classification process are a critical step in deep learning-based Pneumonia diagnosis. At this point, the deep learning method automatically extracts the feature through a

series of iterative steps. The extracted feature is then used to classify the data based on the extracted feature (healthy or pneumonia). Finally, the developed system is evaluated using metrics such as Accuracy, specificity, sensitivity, precision, F1-score and so on.

4. Available datasets

[Table 1](#) is a summary of the systems' available datasets that were evaluated. The properties of the datasets, such as the number of images, classes, size of the images, and availability of the data, are summarized.

4.1. The chest X-ray14 dataset

Chest X-ray14 [19] dataset contains 108,948 images of 32,717 patients which were collected from 1992 to 2015 from Picture Archiving and Communication Systems (PACS). This current version of the database contains 14 diseases. There are 14 different types of chest X-ray-related thoracic diseases in this dataset. (Thickening1, Cardiomegaly;2, Infiltration;3, Cardiomegaly;4, Effusion;5, Nodule;6, Mass;7, Consolidation;8, Pneumonia;9, Fibrosis;10, Pneumothorax;11, Emphysema;12, Edema;13, Hernia;14). This massive data set includes CSV-formatted metadata describing the demographic characteristics of patients, including age and sex. X-ray images of their original size (3000×2000 pixels) were downsized to 1024×1024 without substantial loss of quality or information. CXRs were performed on 63,340 (56.5%) males and 48,780 (43.5%) females, with a mean age of 46.9 years. The provided data set contained fewer than 1500 images of pneumonia.

4.2. Pediatric CXRS for pneumonia detection

There are 5856 images in the chest X-ray database for children ages 1–5 [1]. This dataset was collected from the Guangzhou Women and Children's Medical Centre (Guangzhou, China) which is available on Kaggle. The database has 3 folders in its train, test, and Val. Every one of the three primary folders has normal and pneumonia subfolders. There were 2780 images of bacterial pneumonia, 1493 images of viral pneumonia, and 1583 images of healthy people breathing. The majority of the images are the anterior-posterior position as it is the most common way to detect the disease.

4.3. MIMIC CXR dataset

MIMIC-CXR [20] contains 377,11 images of 14 chest diseases. It is considered the largest publicly available dataset. From 2011–2016, dataset was collected at the Beth Israel Deaconess Medical Center in, Massachusetts, USA. The typical image resolution is 2544×3056 .

4.4. Open-I Indiana dataset

The dataset contains 7470 X-ray images collected through Indiana university and medicine school. The image resolution is 512×512 pixels and it is associated with 3955 reports. Although the collection is accessible to the general public, there are only 40 images of pneumonia. Images of cardiac hypertrophy, pulmonary edema, opacity, and pleural effusion are labeled with the disease perspective (frontal or lateral) and other important information.

4.5. MC dataset

Jaeger et al. collected this dataset by collaborating with Montgomery County's (MC) screening program for tuberculosis (USA) [22]. Among the 138 chest images in the dataset, 63 came from men, 74 from women, and one was from an unidentified patient. Two categories make up the dataset. There were 58 tuberculosis patients and 80 healthy participants. This dataset is publicly available with varying resolutions from 4020×4892 – 4892×4020 pixels. Since it doesn't have any samples of

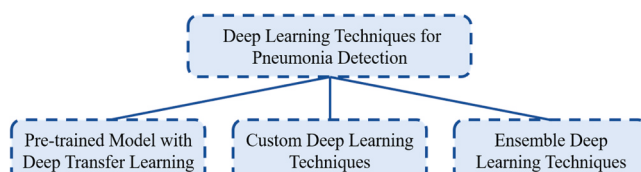


Fig. 1. Taxonomy of Pneumonia diagnosis using deep Learning.

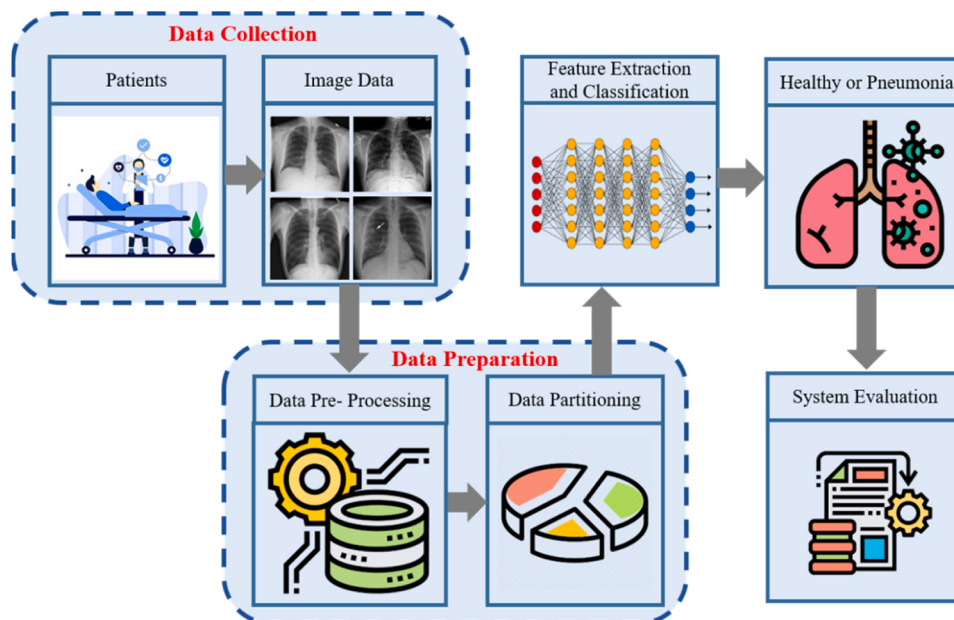


Fig. 2. General flow chart of pneumonia diagnosis using deep learning-based technique.

Table 1

Available Datasets for Pneumonia Diagnosis.

Datasets	Author	Image Modalities	No. of samples	No. of classes	Image size	Accessing State	Reference
Chest X-ray14	Wang et al.	PNG	108,948	8	1024×1024	Public	[19]
Pediatric Chest X-ray	Kermany et al.	JPEG	5856	2	1040×664, 1224×1000, 1848×1632	Public	[1]
MIMIC CXR	A. E. W. Johnson et al.	JPEG, DICOM	377,110	14	2544×3056	Public	[20]
Indiana Dataset	Demner-Fushman et al.	DICOM	7470		512 × 512	Public	[21]
MC dataset	Jaeger et al.	PNG	138	2	4020×4892 4892×4020	Public	[22]
Shenzhen dataset	Jaeger et al.	DICOM	662 images	2	3000×3000	Public	[22]
KIT dataset	Ryoo and Kim et al.		10,848 images				[23]
JSRT dataset	J. Shiraishi et al.	DICOM	247 images	3	2048 × 2048	Public	[24]
RSNA dataset	Radiological Society of North America	DICOM	30,000 images	3	1024×1024	Public	[25]
CXLSeg dataset	Nimalsiri et al.	JPEG	243,324	4	224×224	Public	[26]

pneumonia, it cannot be utilized to detect pneumonia.

4.6. Shenzhen dataset

Jaeger et al. obtained the Shenzhen dataset from the Guangdong Medical College in Shenzhen (Guangdong Province, China). [22]. There are 662 chest x-rays in total, from 326 healthy people and 336 people with tuberculosis. Out of the 662 CXR images, 442 were from men, 213 were from women, and 7 were from people with unknown or other genders. This dataset is publicly available with a resolution of 3000 × 3000 pixels in PNG format. Since it doesn't have any samples of pneumonia, it cannot be utilized to detect pneumonia.

4.7. KIT dataset

Ryoo & Kim, (2014) collected the Kit dataset from the Korea Institute of Tuberculosis. There are a total of 10,848 images, including 7020 from healthy people and 3828 from people with tuberculosis.

4.8. JSRT dataset

The JSRT dataset, which Shiraishi et al., (2000) gathered, consists of 247 images of patients with nodules; the average age of these patients

was 60. Out of 247 images, 100 showed malignant pulmonary nodules, 54 showed benign ones, and 93 showed no nodules at all in the lungs. From these 154 images, 119 belonged to men (68 of whom had nodules and 51 did not), while the remaining 128 were taken by women (86 of whom had nodules and 42 did not). The dataset is 12 bits depth in grayscale and has a dimension of 2048 pixels by 2048 pixels. Since it doesn't have any samples of pneumonia, it cannot be utilized to detect pneumonia.

4.9. RSNA dataset

The 30,000 chest X-rays in the RSNA dataset have annotations for pneumonia (RSNA, 2018). With a resolution of 1024 × 1024, the images are 8-bit in grayscale. Radiologists use bounding boxes to add annotations on lung opacities. Lung opacity, normal, and not normal are the three available classes.

4.10. CXLSeg dataset

The dataset contains 243,324 frontal views of CXR pictures, each with its own segmented mask. Following a comparative investigation of various U-Net versions, the CXR pictures are segmented using a U-Net model with spatial attention (SA-U-Net). The primary MIMIC-CXR

dataset consists of 243,334 frontal pictures from both AP and PA viewpoints. Because there were ten trials with missing reporting, the frontal images for those investigations were omitted when the dataset was created. The segmented dataset maintains the same directory format as its original MIMIC-CXR.

5. Pre-trained model with deep transfer learning

5.1. Transfer learning

The primary objective behind transfer learning is to apply the knowledge gained from addressing one problem to a new but related topic. Pre-trained models are trained on one dataset and are applied to solve problems on another dataset. Numerous pre-trained models can act as the foundation for training a neural network rather than beginning from scratch. The pre-trained CNNs VGG, DenseNet, Inception Net, MobileNet, ResNet, and U-Net are among the most popular ones for analysing medical images. The ImageNet dataset contains 14 million images and 1000 classes used to train these models. The information is transferred between the pre-trained model and the new model in the same domain, it is usual practice to fine-tune the model's higher-level layers while freezing its lower ones shown in Fig. 3. To solve the desired problem, the knowledge acquired from that training is applied.

5.2. Pre-trained models

5.2.1. VGG 16

VGG is a widely used deep convolutional neural network architecture for image recognition. It has two versions: VGG16 and VGG19. VGG16 is made up of sixteen layers, while VGG19 is made up of 19 layers. The ImageNet dataset was used to train this architecture. The VGG16 model achieves around 92.7% accuracy in the top 5 tests on ImageNet. There are about 14 million photos in the dataset, organized into over a thousand categories. The fundamental features of CNN serve as the foundation of VGGNets' architecture. Because of its simplicity and high-performance metrics, many researchers use the VGG-16 pre-trained model for image data analysis. VGG16 consists of 13 convolution layers, 5 pooling layers, and 3 fully connected layers, as shown in Fig. 4. The input image size for VGG16 is 224×224 . Over 140,000,000 parameters give this network its depth. SoftMax is used as the last classifier in the output layer Fig 4.

5.2.2. InceptionNet

An improved version of the well-known GoogleNet [27] model is Inception-v3[28]. Using transfer learning, it has demonstrated promising classification results in a number of biomedical fields. Inception-v3

presented an inception model based on GoogleNet that incorporates three convolutional layers of 5×5 , 3×3 , and 1×1 . The data from each layer is put into a single vector and sent to the next stage of processing. By decreasing the total amount of parameters, this layout simplifies the computation. Fig. 5 depicts Inception-fundamental v3 architecture Fig.5.

5.2.3. ResNet18

ResNet stands for Residual Network, which was introduced in 2015 by Kaiming He in their paper "Deep Residual Learning for Image Recognition." [29]. ResNet was created to address two issues with CNNs: the vanishing gradient issue, in which the gradient reaches 0 and no additional updating of weights occurs, and the degradation problem. Based on factors like activation function, input dimensions, number of layers, etc., there are three different ResNet CNNs. Instead of gaining knowledge from unreferenced functions, ResNet gain knowledge from residual functions in relation to the inputs from the layer. Residual networks don't require that each of the layers stacked on top of each other exactly match a given underlying mapping. Instead, these layers can fit a residual mapping. To construct a network, they stack leftover blocks atop one another.

5.2.4. DenseNet

Convolutional neural networks that use dense connections between layers are known as DenseNet. A number of variations exist, including DenseNet 201 and DenseNet 169. While DenseNet169 only has 169 layers, DenseNet201 has 201 layers. When using dense blocks, which connect all layers directly to each other, the size of the images that come in is 224×224 pixels. In order to maintain the feed-forward nature, each layer is fed additional data from the layers below it and sends its own feature maps to the layers above it. DenseNet201 is an advancement over ResNet. Even though it uses only half as many parameters as Resnet, it achieves comparable accuracy on the ImageNet dataset. By increasing feature reuse, strengthening feature propagation, lowering parameters, and comparing DenseNet to standard networks, performance can be improved.

5.3. Pneumonia detection using transfer learning

Wang et al.[19] collected chest X-ray images of 14 diseases (previously 8). The dataset is obtained from 32,717 patients and contains 108,948 images. Some pre-trained state of the art models (GoogleNet, AlexNet, ResNet and VGG16) were used for classifying the pathologies. Among those pre-trained models, only the ResNet model had given higher accuracy with $AUC=0.63$. Although the accuracy was low, the author did give researchers a starting point by releasing a dataset. Yao

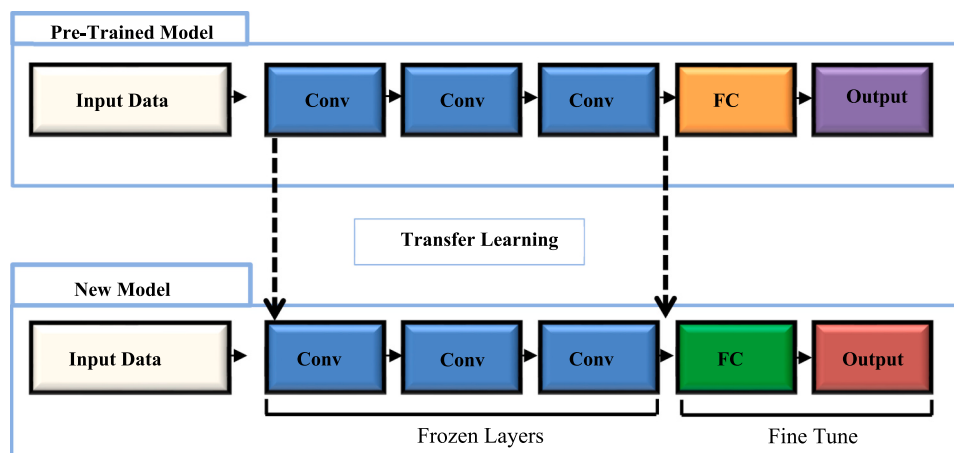


Fig. 3. Concept of Transfer Learning.

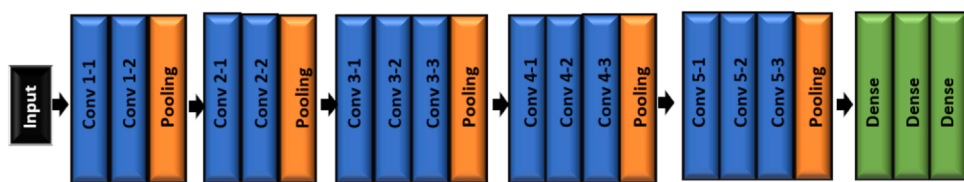


Fig. 4. VGG16 Architecture.

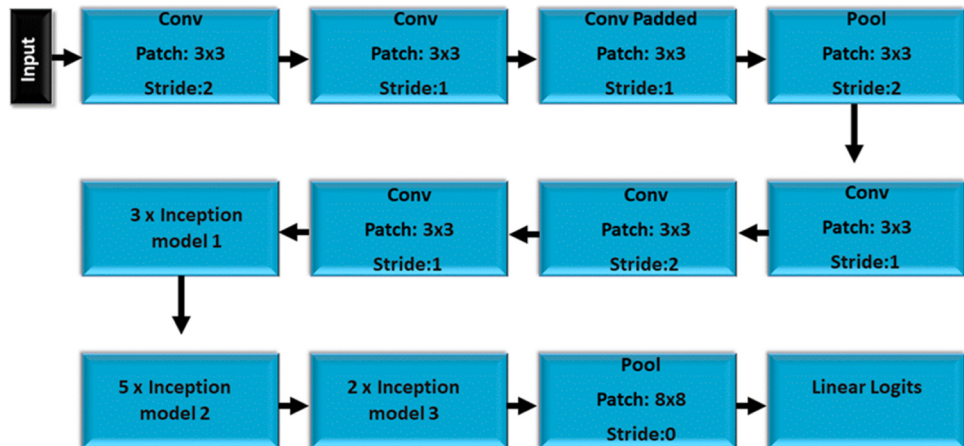


Fig. 5. InceptionNet Architecture.

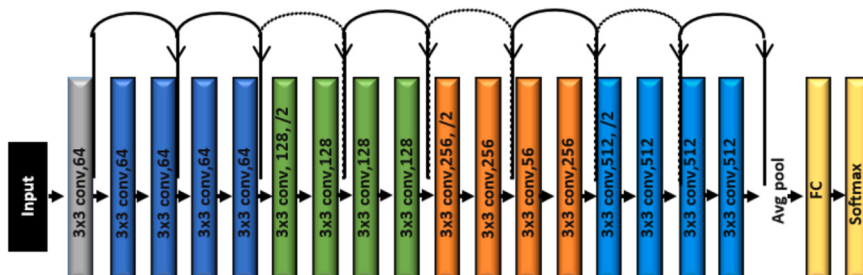


Fig. 6. ResNet18 Architecture.

Table 2

Summary of some well-known pre-trained models.

Model Name	No. of parameters (Millions)	Convolution layers, Pooling layers, fully connected layers	Image size	Model size (in MB)	Depth	Novelty	Limitations
VGG16	138	13,5,2	224×224	527	23	An excellent architecture for gold-standard on specific problem.	Training time is very long.
InceptionNetv3	23.83	99,15,1	299×299,224×224	91	N/A	Factorizing the n*n filters to 1*n and n*1and 7*7 convolution factorization, more quickly and efficiently.	The architecture is very much complicated.
DenseNet201	20	200,5,1	224×224	80	201	Uses features without duplication, shows and has one of the best results for transfer learning.	Each layer's feature maps are combined with the one before it, and the data is repeated several times.
MobileNet	3.4	3(CL),1(PL) and Bottle-necks	224×224	14	88	The computation is very fast and distinguishable convolutions that are depth-wise.	The accuracy is not in satisfactory level.

et al. [8] suggested a model to enhance the accuracy of classification. It was a two-stage end-to-end model with a DCNN encoder and an RNN (long short-term memory) decoder. The DenseNet encoder was created by making certain adjustments to the DenseNet network after it was

trained using the chest X-ray 14 dataset. The proposed model proved improved classification performance with an AUC of 0.71. Kermany et al. [1] suggested a transfer learning system for use in eye diagnosis using optical coherence tomography (OCT). Transfer learning from

retinal OCT pictures formed the backbone of the system used to classify pneumonia in a pediatric CXR dataset [1]. This approach has a 92.8% accuracy rate, a 0.90% specificity rate, and a 0.93% sensitivity rate for normal and pneumonia images, and a 90.7% accuracy rate, a 0.88% specificity rate, and a 0.90% sensitivity rate for identifying bacterial vs. viral pneumonia. Despite the authors' use of a transfer learning approach and the development of a pediatric dataset, the results were unpromising in terms of accuracy and specificity.

Ayan and Ünver, [30] used two different pre-trained networks, Xception and VGG16, to categorize the diseases. He also compared the performance of both networks. The networks were trained and tested using the Pediatric Chest X-ray dataset [1]. The VGG16 network has an accuracy, specificity, and sensitivity of 0.87, 0.91, and 0.82 when comparing normal and pneumonia images, while the Xception network had values of 0.82, 0.76, and 0.85. The model's performance matrices reveal that the VGG16 network excels at normal case detection, while the Xception network excels at pneumonia case detection, but neither network's performance is particularly encouraging and further development is required. Similar dataset was used by Soysal for recognizing thorax diseases applying zero-shot learning [31]. In another work, Hasan et al. [32] utilized VGG16 and ResNet50 model for pneumonia and COVID-19 diagnosis achieving 89.23% and 88.80% accuracy rates for VGG16 and ResNet50 models. Thakur et al. In another work done by Thakur et al. [33] proposed a pre-trained based VGG16 network for pneumonia classification on the Pediatric Chest X-ray [1] dataset. The accuracy, recall, precision, and F-1 score of 90.54%, 98.7%, 87.9%, and 92.9%, respectively. For the purpose of detecting pneumonia, Li et al. [34] suggested a transfer learning-based approach. The proposed architecture for the model was an attention-guided squeeze-and excitation network (SENet). This technique removes the area of the chest X-ray associated with pneumonia and replaces it with pixels that are not associated with pneumonia in order to attract the CNN's attention. For segmentation and classifying the lung regions, U-Net and SENet architecture were used. Results for the suggested models were obtained at a variety of threshold (T) settings. At a threshold of $T(\text{IoU}) = 0.3$, the model achieved a 0.262 accuracy score and a false-positive rate of 0.194. Precision was 0.611 and recall was 0.835. Jain et al. [35] presented multiple deep learning-based approaches for identifying pneumonia in chest X-rays. Two variants were created, one using CNN and the other using CNN, VGG19, VGG16, Inception-v3 and ResNet50. The validation accuracies of the models were 85.26%, 92.31%, 87.28%, 88.46%, 77.56%, and 70.99%, respectively. When compared to the pre-trained model, the customized CNN performed better (92.3% and 98.0% recall). Since there were not enough images to use a standard data division method, the precision was poor. Fernando et al. uses deep learning to evaluate images of chest X-rays and identify normal, pneumonia, and COVID-19 diseases. Experiments were conducted using various deep learning models, including MobileNetV2, Resnet50, InceptionV3, and Xception, with additional layers and 5-fold cross-validation. ResNet50 achieved an average accuracy and recall of 98.87% and 98.54%, respectively [36].

6. Custom deep learning techniques

6.1. Convolutional neural network

"Deep learning networks" are artificial neural networks that have many layers and can handle huge amounts of data. One of the most popular types of deep neural networks is the CNN. Integrating computer vision and deep learning is the main goal of CNN. The convolutional, pooling, fully connected, and non-linearity layers are just a few of the layers of a CNN architecture. In contrast to non-linearity and pooling layers, fully connected and convolutional layers have parameters. When it comes to deep learning issues, the CNN performs quite well with image data such as image classification, segmentation, detection, etc. Fig. 7.

CNN is made up of numerous hidden layers named convolutional

layers, in which a linear function calculates successive convolutions over a picture to extract information. CNN is made up of numerous hidden layers named convolutional layers, in which a linear function calculates successive convolutions over a picture to extract information. It also has a pooling layer like Average Pool or Max Pool to speed up computation by minimizing the image's size. It achieves this by extracting some aspects from the neuron image and eliminating the rest, which enhances the network. In a fully connected (FC) layer, the output is obtained by flattening the total of the outputs from each layer Fig.8.

6.1.1. Convolution layer

A convolutional layer is the linear function that is employed in the CNN architecture. Using image processing feature detectors, every node in the hidden layer extracts a distinct feature. The parameters of the convolutional layer are made up of a set of K learnable filters, or "kernels," where each kernel has a width and a height. Stride convolutions are illustrated using an image in Fig. 9. The main image is at the bottom, and the convolutions' output is at the top. The source image's dimension is decreased as a result of the convolutions.

6.1.2. Pooling layer

Following the calculation of the convolutional layer comes the calculation of the pooling layer. Pooling is done so that the dimensions of the convolutional layer can be reduced even further, and just the features themselves are extracted in order to make the model more accurate. The two types of pooling that are utilized the most frequently are the maximum pooling and the average pooling. The maximum pixel value that can be retrieved from a feature is determined by max pooling, while the average pixel value that can be retrieved from a feature is determined by average pooling. Fig. 10. presents a visual representation of the max and average pooling operation

6.1.3. ReLU activation

ReLU, or rectified linear unit, is a type of activation function. In neural networks, particularly in CNNs, ReLU is the most often employed activation function. The ReLU function is a fundamental calculation that gives an output of either the value given as input directly or 0.0 if the input value is 0.0 or less. When creating most types of neural networks, the ReLU is used as the default. There are some advantages of ReLU activation function. These are: (1) Computational Simplicity. (2) Linear Behavior. (3) Representational Sparsity. (4) Train Deep Networks.

6.2. Pneumonia detection using custom deep learning techniques

Kermany et al. [1] proposed pediatric CXR data set which was used to train a CNN with four convolution layers, as proposed by Stephen et al. [48]. The studies data [1] was split up in different ways. For example, 2134 images went to the validation set, while augmentation methods were used to add to the training dataset. The findings indicate an accuracy of 93.7%. Complex DL model in terms of computation on the validation dataset; However, it was not possible to integrate this performance with other metrics. One major shortcoming of their study is that they did not do any extra testing or evaluate how well their method would function in the case of a nonstandard dataset partition. Based on the pediatric CXR dataset, Raheel [5] suggested an 18-layer customized DCNN. The experimental results demonstrated a 99% sensitivity for the suggested system and its accuracy (94.3%) was 1.6% better than that of [1]. The specificity was 86% which was very low. Verma et al. [49] demonstrated a custom CNN for categorizing lung nodules in CXR images into three groups: pulmonary TB, bacterial pneumonia, and viral pneumonia. To prevent overfitting, augmentation technique used to preprocess the images. The experimental findings showed a 99.01% total accuracy. Omar et al. [50] made a custom CNN architecture for detecting pneumonia from CXRs, and it was accurate 87.65% of the time. Omar's study, however, left out important performance metrics including recall, sensitivity and precision.

Table 3

Summary of Pneumonia Detection using pre-trained model with deep Transfer Learning.

Authors	Data Sources	No. of Images	No. of classes	Partitioning	Techniques	Performance	Limitations
Yao [37]	Chest X-rays14	112,120	8	Training 70 %, Testing 20 % and validation 10 %	LSTM and CNN	AUC=0.71	accuracy is low.
Kermany [1]	Pediatric chest X-rays	5856	2		Transfer Learning	accuracy, sensitivity, and specificity 92.8 %, 93.1 %, and 90 %, respectively.	Accuracy and specificity are low
Ayan [30]	Pediatric chest X-rays	5856	2	Training 80 %, Testing 10 % and validation 10 %	Transfer learning of Xception and VGG16	VGG16 had an accuracy of 0.87, a specificity of 0.82, and a sensitivity of 0.90, while Xception's was 0.82, a specificity of 0.85, and a sensitivity of 0.76.	Poor performance; more work is required.
Thakur[33]	Pediatric chest X-rays	5856	2	Training 80 %, Testing 10 % and validation 10 %	Pretrained VGG16	99.4 % accuracy (recall =98.7 %, accuracy=90.54 %, F1 score=92.9 %, precision=87 %).	There is no context for comparison, accuracy and precision are not impressive.
Li [34]	RSNA pneumonia dataset	30,000 images	3	Test 10 %, Training and validation information not available	U-Net, SE-Resnet for lung segmentation, Post-processing, Data augmentation	T(IoU) recall and precision = 0.835 and 0.611 respectively. FPR and Accuracy = 0.194 and 0.262 respectively.	need human post-processing, and precision may be higher.
Jain [35]	Pediatric chest X-rays	5856	2	Training 80 % and Testing 10 %	VGG19, ResNet50, VGG16, two customized models and InceptionV3	Accuracy of VGG19, ResNet50, VGG16, two customized models and InceptionV3 are 88.46 %,77.56 %,87.28 %,85.26 %,92.31 and 70.99 % respectively.	Accuracy and precision were low.
Chhikara[38]	Pediatric chest X-rays	5856	2	N/A	Modified Inception V3, Pre-processing (gamma correction, JPEG compression, median filtering, CLAHE)	Accuracy, F1-score, precision and recall are 90.01 %,93.2 %,90.7 % and 95.7 % respectively.	Accuracy and precision needs improvement
Schwyzer[39]	Reduced dose CT from 100 patients	3948	2	Training 80 %, Testing 10 % and validation 10 %	Pre-trained ResNet-34	Standard dose: Specificity and sensitivity are 93.8 %,0.923 and 92.9 respectively Reduced dose: Specificity and sensitivity are 93.3 %,0.881 and 71.0 respectively	low Sensitivity
Togacar[40]	Pediatric chest X-rays	5849	2	N/A	Deep feature learning model, VGG19, AlexNet, VGG16 Classification via LDA, LR, SVM, DT	Combining features results in 99.4 % accuracy.	Non-standard data division
Liang [41]	Pediatric chest X-rays	5856	2	Training 90 %, Testing 10 %	49 layers CNN with residual DL architecture	Pretrained on Chest X-rays14, precision=0.891, accuracy=90.05 % and Recall=0.967	Precision needs improvements
Zech [42]	Chest X-rays 14 dataset, IU, MSH	Total 158,323 Chest X-rays 14 contains 112,120, IU contains 3807 and MSH contains 42,369 images		Training 70 %, Testing 20 % and Tune 10 %	DenseNet-121 and ResNet-50, detailed experiments	MSH-NIH model: accuracy, sensitivity, specificity and AUC=0.732, 0.950, 0.706, and 0.931 and respectively in the internal test, and 0.238, 0.974, 0.230 and 0.815 respectively in the external test	The research was limited to frontal radiographs, the performance of the external test was not promising
Putha [43]	CQ dataset	2.5 million images		Training 2.3 million chest X-ray images, Testing CQ2000 dataset and Validation CQ100k dataset	ResNet	Accuracy of 89.0%; a starting point for further study	Diagnoses of pneumothorax and the location of lung lesions need to be more accurate and need to be checked out more.
Yee [44]	Pediatric chest X-rays	5856	2	Training 90 %, Testing 10 %	NN, SVM, KNN as Inception V3 as FE as classifier	A number of Convolutional Neural Network classifiers	Sensitivity was only 83.5 %
Aynaoui [45]	Pediatric chest X-rays and CT	1st dataset contains 5856 images and 2nd dataset contains 231 images	2	Training 60 % and Testing 40 %	Pre-trained models (Inception V3, DenseNet201, VGG19, Xception, VGG16, Inception_ResNet_V2, MobileNet V2, customized CNN and ResNet-50)	Intensity normalization and CLAHE are compared in multi-model pre-processing. With the data augmentations mobileNet V2 and Inception_ResNet_V2, accuracy was about 96 %.	There is absolutely nothing to compare it to. Separation of data and analysis based not on similar work but on pneumonia samples
Ilyas Sirazitdinov [46]	Publicly available RSNA Pneumonia detection challenge dataset.	30,000 images	3	For 1st stage: Training image:25,684 Testing image:1000 For 2nd stage: Training image:25,684 Testing image:3000	RetinaNet And Mask R-CNN	Precision values for RetinaNet and Mask R-CNN for first stage are 0.192 and 0.169, and for second stage are 0.202 and 0.165	Can use other directions rather than x-rays, meta information can be important for further experiments.
Željko KNOK, Klaudio PAP, Marko HRNČIĆ.[47]	Pediatric chest X-rays	5856 images	2	Training set: 90 % of the total image Testing set:10 % of the total image	CNN	Accuracy 94 %	Internet required every time while using this.

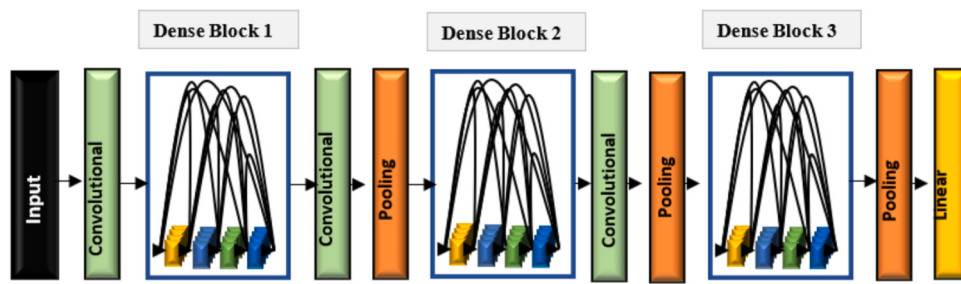


Fig. 7. DenseNet Architecture.

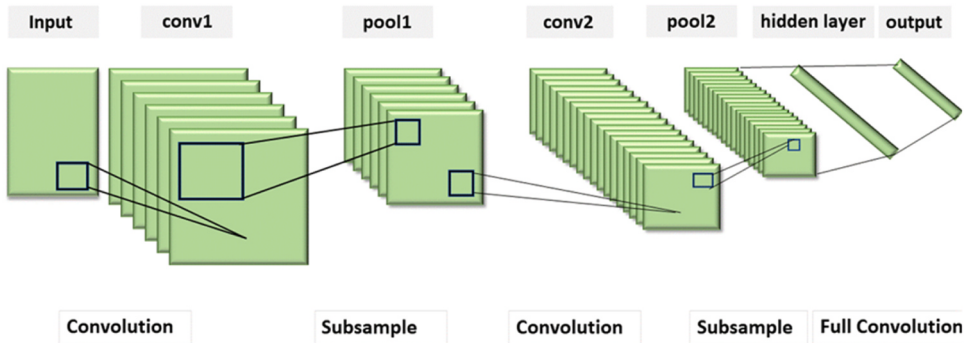


Fig. 8. Typical Architecture of CNN Model.

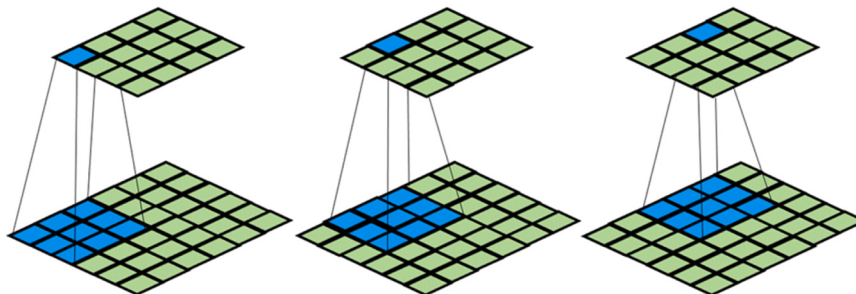


Fig. 9. Convolution Process.

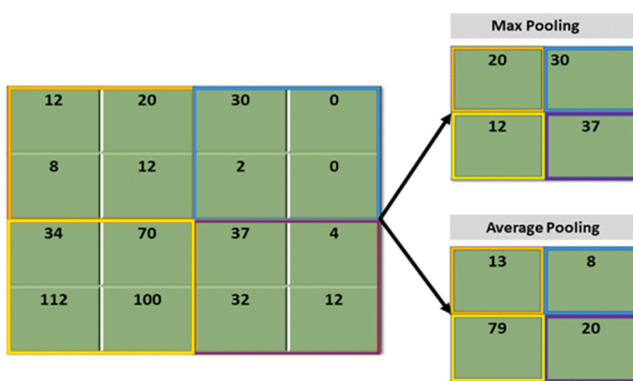


Fig. 10. Pooling Process.

For the categorization of pneumonia from CXRs [1], Bhatt Rushi and Yadav, [51] suggested a nine-layer customized CNN that was computationally inexpensive. Authors got 96.18%, 98.16% sensitivity, and 91.29% specificity after randomly splitting data into sets for training and test. The usual data division suggested in a prior study [1] was not

followed by these authors, and the specificity is also unimpressive. Wu et al. [52] suggested an adaptive median filter CNN and RF (ACNN-RF). The images were first processed with a median filter to get rid of any distracting background noise. A CNN was used to extract features, which were then used by RF to classify the images using GridSearchCV. The results of the experiments showed that the proposed technique had 0.90 precision, 96.9% accuracy, and 0.95 recall. In addition, the proposed system tested in 625.4 seconds as opposed to 921.2 seconds for the CNN model.

A preprocessing technique was suggested by Sarkar Rahul and Hazra, [53] and then a DL model based on CXRs [1] with an accuracy of 98.82% and an AUC of 0.99726. Image enhancement using the CLAHE method, a modified DL model in which the GAP layer replaces the flattened layer, and bilateral filtering are all talked about.

Rajaraman et al. [54] proposed a graphic representation of how CNNs make predictions and activate their networks. Graphics showed the results of an experiment that compared the VGG16 model to a CNN that was built from scratch. Comparing the VGG16's learning and optimization results to those produced using the modified CNN, the VGG16 performed better. From 92.8% in Kermany et al. [1] to 96.2% with the VGG16, the accuracy of differentiating between pneumonia and normal pictures was enhanced. The accuracy of differentiating

between bacterial and viral pneumonia increased from 90.7 % to 93.6 % over this time. Although encouraging results were obtained, the VGG16 network's specificity for differentiating between viral and bacterial pneumonia was only 85.9 %.

Abiyev [55] offered customized CNN, CpNN with unsupervised learning, and BpNN with supervised learning for the purpose of pathology detection in chest X-rays. As compared to VGG19 (92 %), CpNN (80.04 %), VGG16 (86 %), BPNN (89.57 %), VGG19 (92 %), and CNN with GIST (92 %), the suggested CNN achieves greater accuracy (92.4 %). The precision, though, is bound to get better. Hasan provided a simple CNN architecture for pneumonia detection. The proposed model achieved an accuracy of 96 % [56].

7. Ensemble deep learning techniques

7.1. Ensemble learning

Ensemble learning refers to a group of methods that integrate several inducers to reach a conclusion. An inducer is an algorithmic approach

that takes an input of labelled instances and outputs a model from which those instances can be derived. Predictions for new, unlabeled instances can be made using the created model. Any machine learning technique, including decision trees, linear regression models, neural networks, and more, can be used as an ensemble inducer. The main idea behind ensemble methods is that by combining multiple models, the flaws of one inducer will likely be made up for by those of others. This will lead to better performance than if only one inducer was used. Ensemble learning is frequently highly effective when the computing cost of the collaborating inducers is minimal. For solving many machine learning problems, ensembles are now thought to be the most cutting-edge strategy.

7.1.1. AdaBoost

AdaBoost is one of the most widely used dependent techniques for creating ensemble models. The primary objective of AdaBoost is to train new inducers by concentrating on cases that have been previously misclassified. In the training part, the amount of emphasis supplied is based on a weight that is applied to each instance. At the initial iteration,

Table 4
Summary of Pneumonia Detection using Custom Deep Learning Techniques.

Authors	Data Sources	No. of Images	No. of classes	Partitioning	Techniques	Performance	Limitations
Stephan [48]	Pediatric chest X-rays[1]	5856	2	Training 63.5 % and Validation 36.5 %	CNN with four convolution layers	Accuracy 93.7 %	Only accuracy was assessed.
Raheel [5]	Pediatric chest X-rays[1]	5856	2	Training 89.7 %, Testing 10 % and Validation 0.3 %	Deep Convolutional Neural Network (DCNN) of 18 layers	Accuracy 94.3 %, Sensitivity 99.0 %, Specificity 88 %	Specificity has poor performance metrics.
Verma [49]	Shenzhen dataset and Pediatric chest x-rays	1st dataset contains 662 images where 2nd dataset contains 5232 images	2	Validation 30 % Training and testing information not available	Data augmentation and learning rate variation	Overall accuracy 99.01 %	Bacterial pneumonia diagnosis with poor precision
Omar [57]	Pediatric chest x-rays[1]	5856	2	Training 90 % and Testing 10 %	CNN with five convolution layers	Accuracy 87.65 %	Accuracy has poor performance metrics and other performance metrics like precision, Sensitivity, Specificity were not evaluated
Bhatt (Bhatt Rushi and Yadav, 2020)	Pediatric chest x-rays[1]	5863	2	Training 70 %, Testing and validation 30 %	Customized nine-layer CNN	96.18 % Accuracy, 98.16 % Sensitivity, and 91.29 % specificity respectively	Specificity and accuracy need to be improved; data division was not standard
Wu H [52]	Pediatric chest x-rays[1]	5863	2	Training 66.7 % and Testing 32.8 %	Image enhancement, CNN-RF, GridSearchCV-based RF	Accuracy, precision and specificity were 97 %, 90 % and 95 % respectively	Precision needs to be improved; data division was not standard
Sarkar Rahul (Sarkar Rahul and Hazra, 2020)	Pediatric chest x-rays[1]	5856	2	N/A	Image enhancement by CLAHE algorithm and bilateral filtering. Model visualization using Grad-CAM, saliency map	Accuracy, AUC, sensitivity and specificity were 98.82 %, 0.99726, 99.27 % and 95.55 % respectively	Data division was not standard
Rajaraman [54]	Pediatric chest x-rays[1]	5856	2	Training=90 % and Testing=10 %	Deep Convolutional Neural Network (DCNN) and Atlas-based detection algorithm	Accuracy and specificity were 96.2 % and 85.9 % respectively	Specificity needs to be improved
R.H. Abiyev [55]	Chest x-rays14	1,08,948 images	8	Training 70 % and Validation 30 %	CpNN, BpNN and CNN	Accuracy 92.4 %, VGG16 (86 %), VGG19 (92 %), CpNN (80.04 %), BpNN (89.57 %), CNN using GIST (92 %)	CNN converges more slowly than CpNN, Accuracy needs to be improved
Chakraborty [58]	Pediatric chest x-rays[1]	5856 images	2	N/A	17 layers network with three convolutional layer CNN	Accuracy, recall, precision was 95.62 %, 96 % and 95 % respectively	
Hasan [56]	Pediatric chest x-rays	5856 images	2	Training 80 %, test and validation 20 %	CNN with three convolution layers	Accuracy, precision, recall and F1-score score were 96.24 %, 94.19 %, 91.82 % and 92.98 % respectively.	

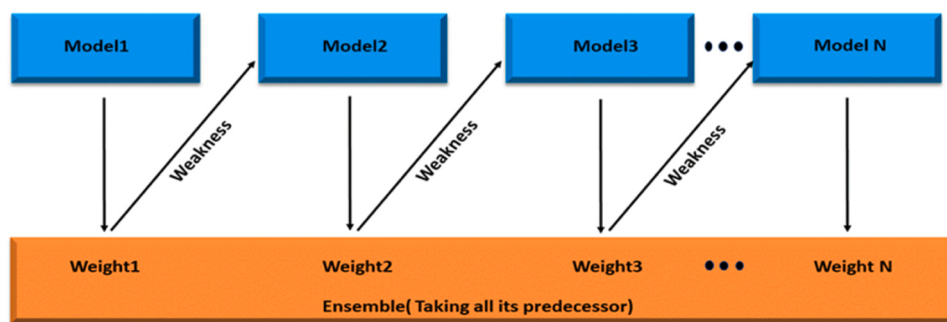


Fig. 11. AdaBoost Ensemble Technique.

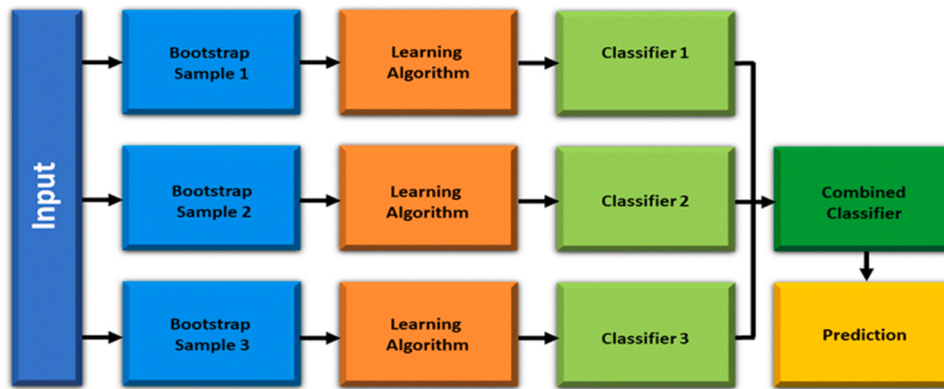


Fig. 12. Bagging Ensemble Technique.

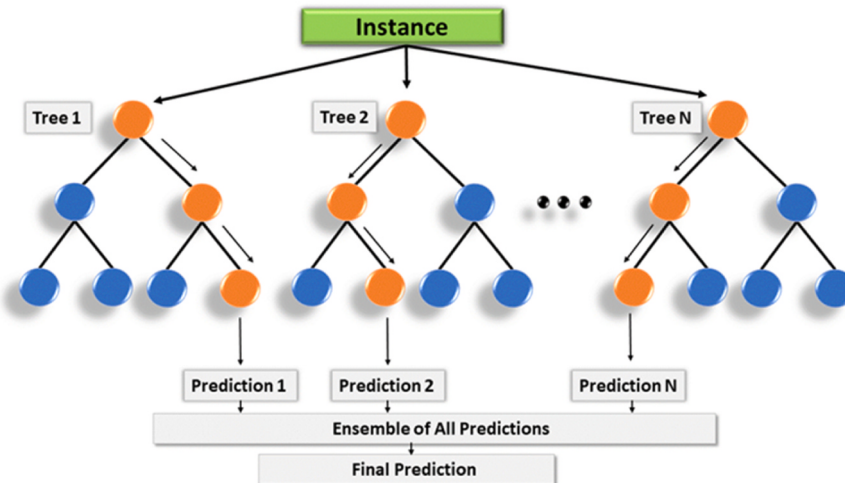


Fig. 13. Random Forest and Random Subspace Technique.

each instance is given the same weight. The weights of instances that are incorrectly classified are increased with each iteration, whereas the weights of instances that are successfully classified are dropped. Additionally, on the basis of their total prediction performance, weights are given to the distinct base learners.

7.1.2. Bagging

Bagging is a quick and efficient method for creating an ensemble of individual models. Here, a subset of instances from the entire dataset is used to train each inducer. Most of the time, a sample has the same number of occurrences as the whole dataset. This makes sure that there are enough examples of each inducer. The ultimate prediction of an

undiscovered instance is chosen by majority voting among the inducers' predictions. While we train the same inducer, a few original instances appear multiple times, while other examples might not be included at all because sampling is done using replacements. Due to the independent training of the inducers, bagging may be readily accomplished in parallel by training every inducer with a distinct processing unit.

7.1.3. Random forest and random subspace methods

Amit and Geman, [59] and Ho, [60] separately introduced random forest at roughly the same time. Because of its predictive performance and simplicity, random forest is becoming more popular. Also, compared to other approaches like GBM that need careful tuning,

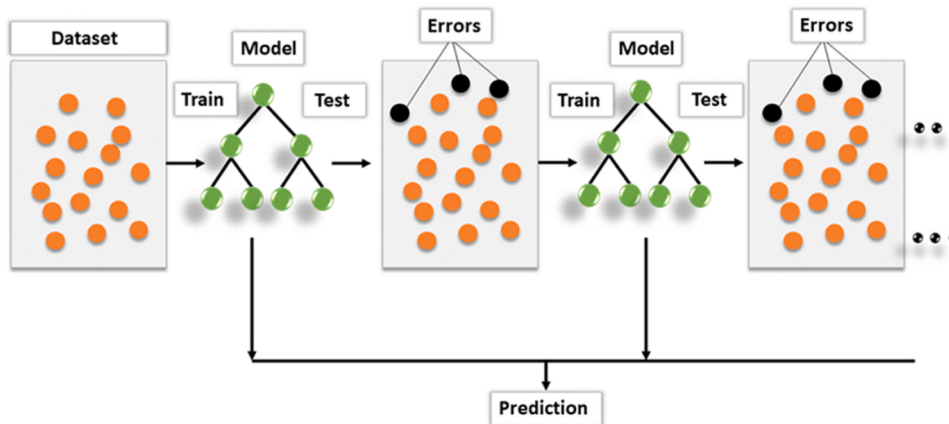


Fig. 14. Gradient Boosting Ensemble Technique.

random forest is seen to be very simple to tune. Many independent and unpruned decision trees are used in random forest. Two randomization procedures are used to introduce randomness into the decision tree inducers: (a) Use different instances of the sample to train each tree. (b) Instead of selecting the ideal split for each node, the inducer will select the best split among a subset of the attributes randomly.

7.1.4. Gradient boosting

Each inducer's training of gradient boosting machines is reliant upon the training of previously trained inducers [61]. The primary distinction between other methods and GBM is that with GBM, function space optimization is used. It also has a learning process whose objective is to build base learners with the highest possible correlation with the loss function's associated negative gradient over the entire ensemble [62]. To create a loss function that can be arbitrarily differentiated, GBM generates a succession of regression trees, each of which makes predictions about the pseudo-residuals of the trees that came before it. In order to use an arbitrary loss function, the user must specify its specification so that the associated negative gradient can be calculated. Each new model is trained to make the loss function smaller, which makes the predictions more and more accurate over time. When comparing a GBM model to a random forest, the latter often has fewer shallow trees. For the GBM model, it is necessary to choose the optimum number of trees. Because making it too low or too high may cause underfitting or overfitting, respectively. To get around this, a validation set is used to measure how well the model predicts overall and figure out the best number of repetitions.

7.2. Pneumonia detection using ensemble learning

In order to detect pneumonia from pediatric CXRs, Chouhan et al. [63] presented an ensemble of Inception v3, DenseNet-121, ResNet, AlexNet and GoogleNet models. The ensemble technique outperformed the other methods, according to numerous experiments, obtaining sensitivity and accuracy of 99.0% and 96.4% respectively.

CXR problems (cardiomegaly and tuberculosis) can be accurately identified with the use of ensemble DCCN models presented by M. T. Islam et al. [64]. (AlexNet, VGG16, ResNet-50, VGG19, ResNet-152 and ResNet-101). When compared to rule-based methods, the ensemble DCCNs showed a 17% improvement in the accuracy of diagnosing cardiomegaly and tuberculosis in the JSRT, Indiana, and Shenzhen datasets. The proposed ensemble model performed well, although it had a low sensitivity of 88% for tuberculosis diagnosis and a low specificity of 92% for cardiomegaly detection. The outcomes need to be improved.

For the purpose of detecting and localizing pneumonia using the RSNA dataset, Sirazitdinov et al. [65] developed an ensemble of mask-R-CNN and RetinaNet. The ensemble's precision, F1 score, and

recall were, respectively, 0.75, 0.77, and 0.70. The experimental results show that, when compared to the outcomes of the models (for ResNet-50 and DenseNet-121 the F1 score was 0.68 and 0.731 respectively), the suggested ensemble model performed better. Although in case of confusion matrix FP and FN needs to be minimized.

To extract features from CXRs, Ko et al. [63] presented a weighted ensemble combining RetinaNet and mask-R-CNN. The weighted ensemble of three RetinaNet models and two mask R-CNNs models produced the best results, with a mean average precision of 0.21746 as opposed to the individual model's 0.19984 although the authors did not make any comparison with the already published work.

In order to distinguish pneumonia from CXRs [1], Hashmi presented a weighted classifier made up of the DL models Xception, InceptionV3, ResNet18, MobileNetV3 and DenseNet121.700 test images were used where 400 for pneumonia cases and 300 for normal cases [66]. A high accuracy of 98.43%, as well as precision and recall values of 98.26% and 99.0%, were confirmed by the trial results. Similarly, Hasan et al. [67,68] proposed weighted ensemble of InceptionV3, MobileNetV2, VGG16 and DenseNet169 and Xception models to identify pneumonia and normal cases applying transfer leaning concept and acquired great performance of 92% accuracy.

A DL-based CGNet model was used by Yu et al. [69] to classify pneumonia from CXR [1]. The authors initially retrieved features using a pre-trained DL-based model, and then they used Euclidean distance to reconstitute the features based on their association. Finally, classification using ANN with the reconstructed features produced results with an accuracy of 98.7%, sensitivity of 0.99, and specificity of 0.98. Kumarasinghe et al. emphasize using a modified U-Net architecture form to segment chest X-rays and then classifying the segmented pictures to evaluate the impact on performance. With the suggested modified U-Net architecture, we achieved a 93.53% intersection over union and 99.83% accuracy in segmentation-aided ensemble classification [70].

Rajaraman et al. [71] used three datasets named CheXpert, TBX11K, RSNA for pneumonia detection. The authors tried different combination of classifier backbones and weight initializations. But the best outcomes got from the ensemble of (ResNet-50 with chest X-ray image modality-specific weights + focal loss, ResNet-50 with chest X-ray image modality-specific weights + focal Tversky loss, and ResNet-50 with random weights + focal loss). In terms of the mAP measure (0.3272, 95 % CI: (0.3006,0.3538)), the ensemble of the top three RetinaNet models outperformed individual models. The results surpass the state of the art (mAP: 0.2547).

8. Discussion and future scope

Chest radiography is very important for the diagnosis and treatment of disorders related to the chest. As a result, automatic detection and

Table 5

Summary of Pneumonia Detection using Ensemble Learning.

Authors	Data Sources	No. of Images	No. of classes	Partitioning	Techniques	Performance	Limitations
Chouhan [72]	Pediatric Chest X-ray	5856	2	Training 90 % and Test 10 %	Ensemble (Inception v3, ResNet, AlexNet, GoogleNet and DenseNet–121)	Accuracy, sensitivity and precision was 96.4 %, 99.0 % and 93.2 % respectively	Precision needs to be improved. Computationally challenging.
Islam [64]	Indiana Dataset [21], Shenzhen dataset [22] and JSRT	1st,2nd and 3rd dataset contain images of 7284,662 and 247 images respectively	2nd and 3rd dataset contain classes of 2 and 3 respectively	N/A	Ensemble DCNN (VGG16, V6619, AlexNet, ResNet–101, ResNet–152, ResNet–50)	for detecting cardiomegaly accuracy 93 % and specificity 92 %. And for tuberculosis accuracy 90 % and sensitivity 88 %	Sensitivity needs to be improved for tuberculosis.
Sirazitdinov [65]	RSNA	26,684	3	Training 90 % and validation 10 %	Ensemble (RetinaNet and mask R-CNN)	Precision, Recall, F1 score were 0.75,0.79 and 0.77 respectively	False positive and false negative needs to be minimized
Ko H [63]	RSNA	26,684	3	N/A	Ensemble (RetinaNet and mask R-CNN)	mAP increases to 0.21746 from 0.19984	Computationally challenging.
Hashmi[66]	Pediatric chest x-rays [1]	5836	2	Training=88.05 % and Testing=11.95 %	Weighted classifier (Xception, Inception v3, ResNet18, MobileNetv3 and DenseNet–121), data augmentation	Accuracy and AUC was 98.43 % and 99.76 respectively	
Yu [69]	Pediatric chest x-rays and CT scan dataset	1st and 2nd dataset contain images of 5856 and 746 respectively	2	For 1st dataset Training 89.07 %, Testing 10.65 % and Validation 0.27 % For 2nd dataset Training 56.97 %, Testing 27.21 % and Validation 15.81 %	CGNet	Accuracy =0.98, Sensitivity=1 and Specificity=0.97	
Sivaramakrishnan	CheXpert, TBX11K, RSNA chest X-rays	CheXpert dataset consists of 223,648 frontal and lateral chest X-ray images where TBX11K and RSNA dataset consists of 223,648 and 11,200 CXR images respectively.		For modality-specific retraining CheXpert and TBX11K dataset has been used: 70 % for training, 20 % for testing and 10 % for validation. For RetinaNet based object detection RSNA dataset has been used: 70 % for training, 20 % for testing and 10 % for validation.	Ensemble of 3 models (ResNet–50 with chest X-ray image modality-specific weights + focal loss, ResNet–50 with chest X-ray image modality-specific weights + focal Tversky loss, and ResNet–50 with random weights + focal loss)	The mean average precision (mAP) measure (0.3272, (0.3006,0.3538))	The authors primarily looked at the impact of using classifier backbones specific to the CXR modality in a RetinaNet-based computer vision applications model to enhance consistent pneumonia detection results.
S. Rajaraman [71]	RSNA	26,684	2 classes		Ensemble of 3 models (customized CNN, VGG16, VGG19)	For majority voting the mean accuracy, F, MCC were 97.8, 98.5 and 94.5 respectively. For averaging the mean accuracy, AUC, F, MCC were 98.5, 100.0, 99.0 and 96.4 respectively. For weighted averaging the mean accuracy, AUC, F, MCC were 98.7, 100.0, 99.1, 96.8 respectively.	
Khalid El Asnaoui. [73]	Chest X-ray and CT dataset, Covid Chest X-ray dataset	First dataset contains 5856 images where second dataset contains 231 images only.	4 classes	80 % for training and 20 % for testing	Ensemble of 3 models (InceptionResNet_V2, MobileNet_V2, ResNet50)	The ensemble performance in terms of accuracy, sensitivity, specificity, precision and F1 were 95.09, 94.43, 98.31, 95.53 and 94.84 respectively.	

(continued on next page)

Table 5 (continued)

Authors	Data Sources	No. of Images	No. of classes	Partitioning	Techniques	Performance	Limitations
Enes Ayan et al.	Pediatric Chest X-ray				Ensemble of ResNet-50, MobileNet and Xception model.	The accuracy, sensitivity, specificity and AUC were 95.83, 97.76, 92.73 and 95.21 respectively.	

diagnosis have gained popularity as a research area in computer vision using medical images. There have been several algorithms created using different methods, and a literature review that summarizes the current methods is very much needed. In this study, we tried to give an overview of all the publicly available datasets that have been used to identify pneumonia and the computational complexity, goodness, and usability of the current techniques used by different authors in their research.

In the majority of cases, the chest x-ray datasets [1,4], and [20] are badly imbalanced, and some authors drew conclusions based on limited images from the dataset. So, we draw the conclusion that their findings are untrustworthy and suggest against using their research on a large scale because doing so could endanger patients' lives. It is preferable to use massively scaled data that is balanced and has a million images of pneumonia. Different augmentation technique can be used for the purpose. For this, a variety of augmentation techniques may be employed.

Finally, a large number of studies on pneumonia detection have concentrated on employing custom CNN, pre-trained models, and ensemble learning techniques, where researchers mostly used the pediatric chest X-ray [1] dataset. Here are the most important problems that will need to be fixed in the near future:

- Most previous studies have only employed frontal radiographs. But the use of lateral-view radiography has been shown to increase the accuracy of pneumonia detection [14].
- For the most part, DL algorithms have been the focus of pneumonia detection research. But preprocessing approaches, such as data augmentation and image enhancement, should be addressed to enhance the predictive performance of DL algorithms
- Most ML-based methods for identifying pneumonia don't mention their data-splitting methodology. The research must explain how they chose the training/testing ratio.

9. Limitation of the study

The goal of this study is to look at and present some popular deep learning-based X-ray image-based pneumonia detection methods. Even though many of the key points from the relevant literature have been highlighted, there are still some caveats that need to be worked out in subsequent research. First of all, only deep learning-based algorithms for diagnosing pneumonia are discussed, and background information on deep learning is not specifically covered. Second, for custom architectures, details such as the learning rate, number of layers, batch size, number of epochs, dropout layer, optimizer, and loss function are not covered here; the reader is encouraged to look up these topics in other references. Third, in the majority of cases, the chest x-ray datasets [1,4], and [20] are badly imbalanced, and some authors drew conclusions based on limited images from the dataset. So, we draw the conclusion that their findings are untrustworthy and suggest against using their research on a large scale because doing so could endanger patients' lives. It is preferable to use massively scaled data that is balanced and has a million images of pneumonia. Different augmentation technique can be used for the purpose. For this, a variety of augmentation techniques may be employed. Moreover, many studies do not give any codes that mimic the most important outcomes in the studied pneumonia diagnosis systems.

10. Conclusion

When it comes to diagnosing and treating chest conditions, chest radiography is crucial. As a result, automatic detection and diagnosis have gained popularity as a research area in computer vision using medical images. There have been several algorithms created using different methods, and a literature review that summarizes the current methods is very much needed. In this study, we tried to give an overview of all the publicly available datasets that have been used to identify pneumonia and the computational complexity, goodness, and usability of the current techniques used by different authors in their research.

Research fund

This work was not supported by any research grant.

CRediT authorship contribution statement

Sheikh Md. Rabiul Islam: Writing – review & editing, Supervision. **Shah Muhammad Azmat Ullah:** Writing – review & editing, Validation, Supervision, Methodology, Investigation, Formal analysis. **Md. Rabiul Hasan:** Writing – original draft, Visualization, Validation, Software, Methodology, Investigation, Formal analysis, Data curation, Conceptualization.

Declaration of Competing Interest

The authors declare no conflicts of interest.

Data Availability

No data was used for the research described in the article.

Acknowledgment

The authors wish to thank Dept. of Electronics and Communication Engineering staff and all professors of this department for sporting equipment and other facilities. Thanks to the authors [10] are inspired us to write this review research paper.

References

- [1] D.S. Kermany, et al., Identifying medical diagnoses and treatable diseases by image-based deep learning, *Cell* vol. 172 (5) (Feb. 2018) 1122–1131.e9, <https://doi.org/10.1016/j.cell.2018.02.010>.
- [2] M.M. Islam, F. Karay, R. Alhajj, J. Zeng, A review on deep learning techniques for the diagnosis of novel coronavirus (COVID-19), *IEEE Access* vol. 9 (2021) 30551–30572, <https://doi.org/10.1109/ACCESS.2021.3058537>.
- [3] WHO | World Health Organization. <https://www.who.int/> (accessed Jun. 14, 2022).
- [4] X. Wang, Y. Peng, L. Lu, Z. Lu, M. Bagheri, and R.M. Summers, ChestX-ray8: Hospital-scale Chest X-ray Database and Benchmarks on Weakly-Supervised Classification and Localization of Common Thorax Diseases.” [Online]. Available: <https://uts.nlm.nih.gov/metathesaurus.html>.
- [5] R. Siddiqi, 2019, Automated Pneumonia Diagnosis Using a Customized Sequential Convolutional Neural Network, in Proceedings of the 2019 3rd International Conference on Deep Learning Technologies, in ICDLT 2019, New York, NY, USA: Association for Computing Machinery, 2019, pp. 64–70. doi: 10.1145/3342999.3343001.

- [6] M. Mardani, et al., Deep generative adversarial neural networks for compressive sensing MRI, *IEEE Trans. Med Imaging* vol. 38 (1) (Jan. 2019) 167–179, <https://doi.org/10.1109/TMI.2018.2858752>.
- [7] A. Oates, et al., Shortage of paediatric radiologists acting as an expert witness: position statement from the British Society of Paediatric Radiology (BSPR) National Working Group on Imaging in Suspected Physical Abuse (SPA), in: *Clinical Radiology*, vol. 74, W.B. Saunders Ltd, 2019, pp. 496–502, <https://doi.org/10.1016/j.crad.2019.04.016>.
- [8] L. Yao, E. Poblenz, D. Dagunts, B. Covington, D. Bernard, and K. Lyman, Learning to diagnose from scratch by exploiting dependencies among labels, Oct. 2017, [Online]. Available: <http://arxiv.org/abs/1710.10501>.
- [9] L.L.G. Oliveira, S.A. e Silva, L.H.V. Ribeiro, R.M. de Oliveira, C.J. Coelho, A. L. S. Ana Lúcia, Computer-aided diagnosis in chest radiography for detection of childhood pneumonia, *Int J. Med. Inf.* vol. 77 (8) (Aug. 2008) 555–564, <https://doi.org/10.1016/j.ijmedinf.2007.10.010>.
- [10] W. Khan, N. Zaki, L. Ali, 2021, Intelligent Pneumonia Identification from Chest X-Rays: A Systematic Literature Review, *IEEE Access*, vol. 9, Institute of Electrical and Electronics Engineers Inc., pp. 51747–51771, 2021. doi: 10.1109/ACCESS.2021.3069937..
- [11] W. Khan, N. Zaki, L. Ali, 2020, Intelligent Pneumonia Identification from Chest X-Rays: A Systematic Literature Review*, doi: 10.1101/2020.07.09.20150342..
- [12] Shallu, R. Mehra, Breast cancer histology images classification: Training from scratch or transfer learning? *ICT Express* vol. 4 (4) (Dec. 2018) 247–254, <https://doi.org/10.1016/j.icte.2018.10.007>.
- [13] V. Badrinarayanan, A. Kendall, R. Cipolla, SegNet: a deep convolutional encoder-decoder architecture for image segmentation, *IEEE Trans. Pattern Anal. Mach. Intell.* vol. 39 (12) (Dec. 2017) 2481–2495, <https://doi.org/10.1109/TPAMI.2016.2644615>.
- [14] P. Rajpurkar et al., CheXNet: Radiologist-Level Pneumonia Detection on Chest X-Rays with Deep Learning, Nov. 2017, [Online]. Available: <http://arxiv.org/abs/1711.05225>.
- [15] M. Wainberg, D. Merico, A. Delong, B.J. Frey, Deep learning in biomedicine, *Nat. Biotechnol.* vol. 36 (9) (Oct. 2018) 829–838, <https://doi.org/10.1038/nbt.4233>.
- [16] A. Esteva, et al., A guide to deep learning in healthcare, *Nat. Med.* vol. 25 (1) (Jan. 2019) 24–29, <https://doi.org/10.1038/s41591-018-0316-z>.
- [17] H. Chen, O. Engkvist, Y. Wang, M. Oliverecuna, T. Blaschke, The rise of deep learning in drug discovery, *Drug Discov. Today* vol. 23 (6) (Jun. 2018) 1241–1250, <https://doi.org/10.1016/j.drudis.2018.01.039>.
- [18] D. Shen, G. Wu, H.-I. Suk, Deep learning in medical image analysis, *Annu Rev. Biomed. Eng.* vol. 19 (Jun. 2017) 221–248, <https://doi.org/10.1146/annurev-bioeng-071516-044442>.
- [19] X. Wang, Y. Peng, L. Lu, Z. Lu, M. Bagheri, R.M. Summers, ChestX-ray: hospital-scale chest X-ray database and benchmarks on weakly supervised classification and localization of common thorax diseases, *Adv. Comput. Vis. Pattern Recognit.* (2019), https://doi.org/10.1007/978-3-030-13969-8_18.
- [20] A.E.W. Johnson et al., MIMIC-CXR-JPG, a large publicly available database of labeled chest radiographs, Jan. 2019, doi: 10.48550/arxiv.1901.07042.
- [21] D. Demner-Fushman, et al., Preparing a collection of radiology examinations for distribution and retrieval, *J. Am. Med. Inform. Assoc.* vol. 23 (2) (Mar. 2016) 304–310, <https://doi.org/10.1093/jamia/ocv080>.
- [22] S. Jaeger, S. Candemir, S. Antani, Y.-X.J. Wang, P.-X. Lu, G. Thoma, Two public chest X-ray datasets for computer-aided screening of pulmonary diseases, *Quant. Imaging Med. Surg.* vol. 4 (6) (Dec. 2014) 475–477, <https://doi.org/10.3978/J.ISSN.2223-4292.2014.11.20>.
- [23] S. Ryoo, H.J. Kim, Activities of the Korean Institute of Tuberculosis, Osong Public Health Res Perspect. vol. 5 (S) (Dec. 2014) S43–S49, <https://doi.org/10.1016/J.PHRP.2014.10.007>.
- [24] J. Shiraishi, et al., Development of a digital image database for chest radiographs with and without a lung nodule: Receiver operating characteristic analysis of radiologists' detection of pulmonary nodules, *Am. J. Roentgenol.* vol. 174 (1) (2000) 71–74, <https://doi.org/10.2214/AJR.174.1.1740071>.
- [25] Anouk Stein, MD, Carol Wu, Chris Carr, George Shih, Jamie Dulkowski, Kalpathy, Leon Chen, Luciano Prevedello, Marc Kohli, MD, Mark McDonald, Peter, Phil Culliton, Safwan Halabi MD, Tian Xia. (2018). RSNA Pneumonia Detection Challenge. Kaggle. <https://kaggle.com/competitions/rsna-pneumonia-detection-challenge>.
- [26] W. Nimalsiri, M. Hennayake, K. Rathnayake, T.D. Ambegoda, D. Meedeniya, CXLSeg dataset: chest x-ray with lung segmentation, 2023 Int. Conf. Cyber Manag. Eng. (CyMaEn) (2023) 327–331, <https://doi.org/10.1109/CyMaEn57228.2023.10050951>.
- [27] C. Szegedy et al., Going deeper with convolutions, [cv-foundation.org](https://www.cv-foundation.org), Accessed: Dec. 21, 2022. [Online]. Available: https://www.cv-foundation.org/openaccess/content_cvpr_2015/html/Szegedy_Going_Deeper_With_2015_CVPR_paper.html.
- [28] C. Szegedy, V. Vanhoucke, ... S. I.-P. of the, and undefined 2016, Rethinking the inception architecture for computer vision, [cv-foundation.org](https://www.cv-foundation.org), Accessed: Dec. 21, 2022. [Online]. Available: https://www.cv-foundation.org/openaccess/content_cvpr_2016/html/Szegedy_Rethinking_the_Inception_CVPR_2016_paper.html.
- [29] K. He, X. Zhang, S. Ren, and J. Sun, Deep Residual Learning for Image Recognition." pp. 770–778, 2016. Accessed: Dec. 21, 2022. [Online]. Available: <http://image-net.org/challenges/LSVRC/2015/>.
- [30] E. Ayan, H.M. Ünver, Diagnosis of pneumonia from chest x-ray images using deep learning, *Sci. Meet. Electr. -Electron. Biomed. Eng. Comput. Sci. (EBBT)* (2019) 1–5.
- [31] O.A. Soysal, M.S. Guzel, M. Dikmen, G.E. Bostancı, Common thorax diseases recognition using zero-shot learning with ontology in the multi-labeled chestX-ray14 data set, *IEEE Access* vol. 11 (2023) 27883–27892, <https://doi.org/10.1109/ACCESS.2023.3259062>.
- [32] M.R. Hasan, S.M.A. Ullah, M. Hasan, Deep Learning in Radiology:A Transfer-Learning Based Approach for the Identification and Classification of COVID-19 and Pneumonia in Chest X-ray Images," 2023 Fourth International Conference on Smart Technologies in Computing, Electrical and Electronics (ICSTCEE),pp. (Jul. 2024) 1–6, <https://doi.org/10.1109/ICSTCEE60504.2023.10585226>.
- [33] Y. and A. S and U. R and S.G. Thakur Saurabh and Goplani, Chest X-Ray Images Based Automated Detection of Pneumonia Using Transfer Learning and CNN, in Proceedings of International Conference on Artificial Intelligence and Applications, M. and B. V. E. and S.R. Bansal Poonam and Tushir, Ed., Singapore: Springer Singapore, 2021, pp. 329–335.
- [34] B. Li, G. Kang, K. Cheng, and N. Zhang, Attention-Guided Convolutional Neural Network for Detecting Pneumonia on Chest X-Rays; Attention-Guided Convolutional Neural Network for Detecting Pneumonia on Chest X-Rays. 2019. doi: 10.0/Linux-x86_64.
- [35] R. Jain, P. Nagrath, G. Kataria, V. Sirish Kaushik, D. Jude Hemanth, Pneumonia detection in chest x-ray images using convolutional neural networks and transfer learning, *Measurement* vol. 165 (Dec. 2020) 108046, <https://doi.org/10.1016/J.MEASUREMENT.2020.108046>.
- [36] C. Fernando, S. Kolonne, H. Kumarasinghe, D. Meedeniya, Chest radiographs classification using multi-model deep learning: a comparative study, 2022 2nd Int. Conf. Adv. Res. Comput. (ICARC) (2022) 165–170, <https://doi.org/10.1109/ICARC54489.2022.9753811>.
- [37] L. Yao, E. Poblenz, D. Dagunts, B. Covington, D. Bernard, and K. Lyman, LEARNING TO DIAGNOSE FROM SCRATCH BY EXPLOIT-ING DEPENDENCIES AMONG LABELS." [Online]. Available: <https://openi.nlm.nih.gov>.
- [38] P. G, P. B.T. Chhikara Prateek, Singh, 2020, Deep Convolutional Neural Network with Transfer Learning for Detecting Pneumonia on Chest X-Rays, in Advances in Bioinformatics, Multimedia, and Electronics Circuits and Signals, M. and P. V. and B.V. E. Jain Lakhmi C. and Virvou, Ed., Singapore: Springer Singapore, 2020, pp. 155–168..
- [39] M. Schwyzter, K. Martini, S. Skawran, M. Messerli, T. Frauenfelder, Pneumonia detection in chest x-ray dose-equivalent CT: impact of dose reduction on detectability by artificial intelligence, *Acad. Radio.* vol. 28 (8) (Aug. 2021) 1043–1047, <https://doi.org/10.1016/J.ACRA.2020.05.031>.
- [40] M. Toğacıcar, B. Ergen, Z. Cömert, F. Özyurt, A deep feature learning model for pneumonia detection applying a combination of mRMR feature selection and machine learning models, *IRBM* vol. 41 (4) (Aug. 2020) 212–222, <https://doi.org/10.1016/J.IRBMB.2019.10.006>.
- [41] G. Liang, L. Zheng, A transfer learning method with deep residual network for pediatric pneumonia diagnosis, *Comput. Methods Prog. Biomed.* vol. 187 (Apr. 2020) 104964, <https://doi.org/10.1016/J.CMPB.2019.06.023>.
- [42] J.R. Zech et al., Variable generalization performance of a deep learning model to detect pneumonia in chest radiographs: A cross-sectional study, 2018, doi: [10.1371/journal.pmed.1002683](https://doi.org/10.1371/journal.pmed.1002683).
- [43] P. Putcha et al., Can Artificial Intelligence Reliably Report Chest X-Rays? Radiologist Validation of an Algorithm trained on 2.3 Million X-Rays."
- [44] S.L.K. Yee, W.J.K. Raymond, Sep. 2020, Pneumonia Diagnosis Using Chest X-ray Images and Machine Learning, in ACM International Conference Proceeding Series, Association for Computing Machinery, Sep. 2020, pp. 101–105. doi: 10.1145/3397391.3397412..
- [45] Y. I.A. El Asnaoui Khalid, Chawki, Automated methods for detection and classification pneumonia based on X-ray images using deep learning, in: Y. and A. M., T. L., R.I. Maleh Yassine, Baddi (Eds.), Artificial Intelligence and Blockchain for Future Cybersecurity Applications, Springer International Publishing, Cham, 2021, pp. 257–284, https://doi.org/10.1007/978-3-030-74575-2_14.
- [46] I. Sirazitdinov, M. Kholiavchenko, T. Mustafaev, Y. Yixuan, R. Kuleev, B. Ibragimov, Deep neural network ensemble for pneumonia localization from a large-scale chest x-ray database, *Comput. Electr. Eng.* vol. 78 (Sep. 2019) 388–399, <https://doi.org/10.1016/J.COMPELECEENG.2019.08.004>.
- [47] Ž. Knok, K. Pap, M. Hrnčič, Implementation of intelligent model for pneumonia detection, *Teh. čki Glas.* vol. 13 (4) (Dec. 2019) 315–322, <https://doi.org/10.31803/tg-20191023102807>.
- [48] O. Stephen, M. Sain, U.J. Maduh, D.-U. Jeong, An efficient deep learning approach to pneumonia classification in healthcare, *Healthcare Eng.* vol. 2019 (2019) 4180949, <https://doi.org/10.1155/2019/4180949>.
- [49] D. Verma, C. Bose, N. Tufchi, K. Pant, V. Tripathi, A. Thapliyal, An efficient framework for identification of Tuberculosis and Pneumonia in chest X-ray images using Neural Network, *Procedia Comput. Sci.* vol. 171 (Jan. 2020) 217–224, <https://doi.org/10.1016/J.PROCS.2020.04.023>.
- [50] H. Omar, A.B.-P. Book, and undefined 2019, Detection of pneumonia from X-ray images using convolutional neural network, *researchgate.net*, Accessed: May 29, 2023. [Online]. Available: https://www.researchgate.net/profile/Ozge-Doguc-2/publication/344164531_Using_Dimensionality_Reduction_Techniques_to_Determine_Student_Success_Factors/links/5f577c4b92851c250b9d53c1/Using-Dimensionality-Reduction-Techniques-to-Determine-Student-Success-Factors.pdf#page=186.
- [51] S. and S.J.N. Bhatt Rushi, Yadav, Convolutional Neural Network Based Chest X-Ray Image Classification for Pneumonia Diagnosis, in: J.N. Gupta Shilpi, Sarvaiya (Eds.) Emerging Technology Trends in Electronics, Communication and Networking, Springer Singapore, Singapore, 2020, pp. 254–266.
- [52] H. Wu, P. Xie, H. Zhang, D. Li, M. Cheng, Predict pneumonia with chest X-ray images based on convolutional deep neural learning networks, *J. Intell. Fuzzy Syst.* vol. 39 (2020) 2893–2907, <https://doi.org/10.3233/JIFS-191438>.

- [53] A. and S. K, G.P. Sarkar Rahul, Hazra, A novel method for pneumonia diagnosis from chest X-ray images using deep residual learning with separable convolutional networks, in: D. and B. S., B.S. Gupta Mousumi, Konar (Eds.), Computer Vision and Machine Intelligence in Medical Image Analysis, Springer Singapore, Singapore, 2020, pp. 1–12.
- [54] S. Rajaraman, S. Candemir, G. Thoma, S. Antani, Visualizing and explaining deep learning predictions for pneumonia detection in pediatric chest radiographs, Proc. SPIE, Mar. 2019, <https://doi.org/10.1117/12.2512752>.
- [55] R.H. Abiyev, M.K.S. Ma'aitah, Deep convolutional neural networks for chest diseases detection, J. Health Eng. vol. 2018 (2018) 4168538, <https://doi.org/10.1155/2018/4168538>.
- [56] Md.R. Hasan, S.M.A. Ullah, Md.E. Karim, 2023, An Effective Framework for Identifying Pneumonia in Healthcare Using a Convolutional Neural Network, 2023 International Conference on Electrical, Computer and Communication Engineering (ECCE), pp. 1–6. Feb. 2023, doi: 10.1109/ECCE57851.2023.10101548..
- [57] H. Omar, A.B.-P. Book, and undefined 2019, Detection of pneumonia from X-ray images using convolutional neural network, *researchgate.net*, Accessed: Apr. 14, 2023. [Online]. Available: [https://www.researchgate.net/profile/Ozge-Doguc-2/publication/344164531_Using-Dimensionality-Reduction-Techniques-to-Determine-Student-Success-Factors.pdf#page=186](https://www.researchgate.net/profile/Ozge-Doguc-2/publication/344164531_Using-Dimensionality-Reduction-Techniques-to-Determine-Student-Success-Factors/links/5f577c4b92851c250b9d53c1/Using-Dimensionality-Reduction-Techniques-to-Determine-Student-Success-Factors.pdf#page=186).
- [58] S. Aich, H.-C. Kim, S. Chakraborty, J. Seong Sim, and H.-C. Kim 言, Detection of Pneumonia from Chest X-Rays using a Convolutional Neural Network Architecture. Detection of Pneumonia from Chest X-Rays using a Convolutional Neural Network Architecture. 저자 (Authors). [Online]. Available: (<http://www.dbpia.co.kr/journal/articleDetail?nodeId=NODE08747418>).
- [59] Y. Amit and D. Geman, Randomized Inquiries About Shape; an Application to Handwritten Digit Recognition, 1994.
- [60] K. Ho, The Random Subspace Method for Constructing Decision Forests, 1998.
- [61] J.H. Friedman, Greedy Function Approximation: A Gradient Boosting Machine, 2001.
- [62] A. Natekin, A. Knoll, Gradient boosting machines, a tutorial, Front. Neurorobot vol. 7 (DEC) (2013), <https://doi.org/10.3389/fnbot.2013.00021>.
- [63] H. Ko, H. Ha, H. Cho, K. Seo, J. Lee, 2019, Pneumonia Detection with Weighted Voting Ensemble of CNN Models, in 2019 2nd International Conference on Artificial Intelligence and Big Data (ICAIBD), 2019, pp. 306–310. doi: 10.1109/ICAIBD.2019.8837042.
- [64] M.T. Islam, M.A. Aowal, A.T. Minhz, and K. Ashraf, Abnormality Detection and Localization in Chest X-Rays using Deep Convolutional Neural Networks, May 2017, [Online]. Available: (<http://arxiv.org/abs/1705.09850>).
- [65] I. Sirazitdinov, M. Kholiavchenko, T. Mustafaev, Y. Yixuan, R. Kuleev, B. Ibragimov, Deep neural network ensemble for pneumonia localization from a large-scale chest x-ray database, Comput. Electr. Eng. vol. 78 (Sep. 2019) 388–399, <https://doi.org/10.1016/J.COMPELECENG.2019.08.004>.
- [66] M.F. Hashmi, S. Katiyar, A.G. Keskar, N.D. Bokde, Z.W. Geem, Efficient pneumonia detection in chest x-ray images using deep transfer learning, Diagnostics vol. 10 (6) (Jun. 2020), <https://doi.org/10.3390/diagnostics10060417>.
- [67] R. Hasan, S.M. Azmat Ullah, A. Nandi, A. Taher, Improving Pneumonia Diagnosis: A Deep Transfer Learning CNN Ensemble Approach for Accurate Chest X-Ray Image Analysis., 2023 International Conference on Information and Communication Technology for Sustainable Development, ICICT4SD 2023 - Proceedings (2023) 109–113, <https://doi.org/10.1109/ICICT4SD59951.2023.10303322>.
- [68] M.R. Hasan and S.M.A. Ullah, "Enhancing Pneumonia Diagnosis: An Ensemble of Deep CNN Architectures for Accurate Chest X-Ray Image Analysis," *Lecture Notes in Networks and Systems*, vol. 867 LNNS, pp. 255–269, 2024, doi: 10.1007/978-981-99-8937-9-18.
- [69] X. Yu, S.H. Wang, Y.D. Zhang, CGNet: A graph-knowledge embedded convolutional neural network for detection of pneumonia, Inf. Process Manag vol. 58 (1) (Jan. 2021) 102411, <https://doi.org/10.1016/J.IPM.2020.102411>.
- [70] H. Kumarasinghe, S. Kolonne, C. Fernando, D. Meedeniya, U-net based chest X-ray segmentation with ensemble classification for Covid-19 and pneumonia, Int. J. Online Biomed. Eng. (iJOE) vol. 18 (07) (Jun. 2022) 161–175, <https://doi.org/10.3991/ijoe.v18i07.30807>.
- [71] S. Rajaraman, P. Guo, Z. Xue, S.K. Antani, A deep modality-specific ensemble for improving pneumonia detection in chest X-rays, Diagnostics vol. 12 (6) (Jun. 2022), <https://doi.org/10.3390/diagnostics12061442>.
- [72] V. Chouhan, et al., A novel transfer learning based approach for pneumonia detection in chest X-ray images, Appl. Sci. (Switz.) vol. 10 (2) (Jan. 2020), <https://doi.org/10.3390/app10020559>.
- [73] K. El Asnaoui, Design ensemble deep learning model for pneumonia disease classification, Int. J. Multimed. Inf. Retr. vol. 10 (1) (Mar. 2021) 55–68, <https://doi.org/10.1007/s13735-021-00204-7>.

Md. Rabiul Hasan, Shah Muhammad Azmat Ullah*, Sheikh Md. Rabiul Islam
Dept. of Electronics and Communication Engineering, Khulna University of Engineering & Technology, Bangladesh

* Corresponding author.

E-mail addresses: mdrabiulhasan7890@gmail.com (Md.R. Hasan), azmat@ece.kuet.ac.bd (S.M. Azmat Ullah), robi@ece.kuet.ac.bd (S.Md. Rabiul Islam).